Parameterization of Carrier Mobility Sum in Silicon as a Function of Doping, Temperature and Injection Level: Extension to p-type Silicon

P. Zheng, F. E. Rougieux, D. Macdonald and A. Cuevas

Research School of Engineering, College of Engineering and Computer Science, The Australian National University, Canberra, ACT, 0200, Australia

***Abstract* — Based on contactless photoconductance measurements of silicon wafers, we have determined the sum of electron and hole mobilities as a function of doping, excess carrier concentration, and temperature. By using data measured on n-type silicon wafers with resistivity from 1Ω.cm to 100Ω.cm, we have previously developed a simple mathematical expression to describe the mobility sum as a function of carrier injection, wafer doping and temperature. In this paper, we provide experimental results for p-type silicon wafers from 150K to 450K and show that they are consistent with this parameterization. We show that our parameterization of the mobility sum in silicon is valid for both p- and n-type silicon for various carrier injection, wafer doping and temperature from 150K to 450K. The new parameterization is also an experimental validation of Klaassen's and Dorkel-Leturcq's models under carrier injection at different temperatures.**

***Index Terms*—silicon, charge carrier mobility, temperature and injection dependent, mobility sum**

I. Introduction

An effective way to determine the recombination parameters of defects in silicon is through temperature and injection dependent measurements of the minority carrier lifetime[1]. A convenient implementation of this method is to use a temperature dependent photoconductance measurement setup[2]. However, the conversion of the measured photoconductance into an excess carrier density requires knowledge of the sum of the electron and hole mobilities as a function of temperature, doping, and injection level.

Numerous experimental data on the minority and majority carrier mobility in both *p* and *n*-type silicon over a wide range of temperatures have been published, mostly as a function of the dopant concentration[3-8]. However, data for the electron and hole mobility sum as a function of excess carrier density available to date have only been measured at room temperature[9-12]. Experimental evidence of the simultaneous impact of excess carrier injection and temperature does not exist, apart from our previous parametrization in n-type silicon [13]. In that previous study, we have determined the sum of the electron and hole mobilities as a function of both excess carrier density and temperature in *n*-type silicon wafers and derived an empirical model describing the mobility. The mobility sum was determined using a recently developed technique [14], which involves comparison of transient and quasi-static photoconductance measurements.

However there is no *p*-type data to validate this new empirical model experimentally as a function of injection level at other temperatures. Moreover it is known that because of the different charge state of donors and acceptors, their scattering potential can, in principle, be different. It is therefore necessary to confirm that the previously established model can be applied to p-type silicon. In this paper, we provide experimental data for *p*-type silicon wafers of resistivity 0.75Ω.cm and 10Ω.cm as a function of injection level and temperature from 150 to 450K. We will show that the *p*-type data is consistent with the new empirical model.

II. Experimental Methods

The samples used in this study were p-type crystalline boron doped silicon wafers. We used two Czochralski-grown wafers of resistivity 0.75Ω.cm and 10Ω.cm. The samples were prepared by damage etching and RCA cleaning, followed by surface passivation at 400°C with plasma-enhanced chemical vapour-deposited silicon nitride films.

The minority carrier lifetime was measured using a calibrated photoconductance tester from Sinton Instruments. In order to measure the simultaneous temperature and injection dependence of the mobility we used a purpose-built, temperature-controlled inductive coil photoconductance instrument [2]. The mobility sum is determined by comparing transient PhotoConductance Decay (PCD) and Quasi-Steady State PhotoConductance (QSSPC) measurements of the excess conductance ($\Delta\sigma$) for every sample. More details of the method can be found in reference [14]. To obtain accurate measurements using this technique, sufficient low surface recombination velocity (SRV) is required to ensure a uniform excess carrier profile. The values of SRV, calculated using the Auger limit from Richter et al [15], ranged from 20cm.s^{-1} to 40cm.s^{-1} for all samples. Based on the measured SRV, computer simulations [16], show that the difference of excess carrier

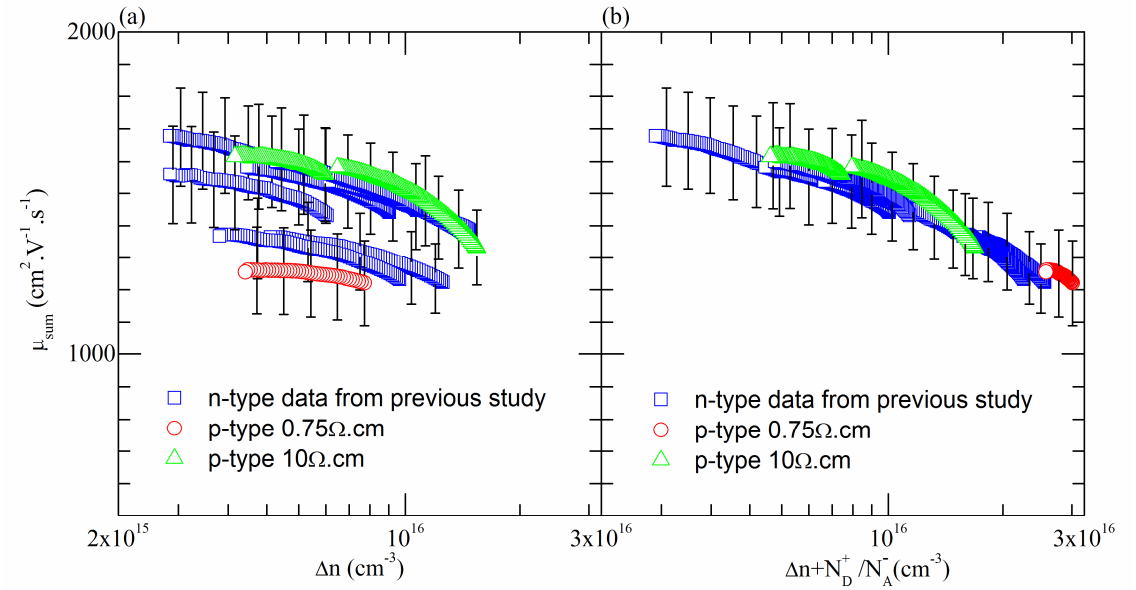

Fig. 1. (a) Measured mobility sum as a function of excess carrier density at 30°C for five n-type and two p-type samples. (b) Measured mobility sum as a function of the sum of excess carrier density and the ionized doping density at 30°C.

density between the front and back surfaces is less than 10% for all the samples, which is sufficient for the measurement. The uncertainty of the mobility sum is estimated by assuming a ±3% uncertainty in the measurement of the generation rate (required for the QSSPC method) and an uncertainty of ±5% in the measurement of the conductance Δσ [17].

III. Results

In Fig. 1(a) shows the mobility sum $\mu_{sum} = \mu_n + \mu_p$ at 30°C as a function of excess carrier density for the five different dopant concentration *n*-type samples ranging from 4×10^{13} cm^{-3} to 1×10^{16} cm^{-3} and two *p*-type samples with dopant concentrations of 1.3×10^{15} cm^{-3} and 2×10^{16} cm^{-3}. At a given excess carrier density, the mobility sum decreases with the dopant density. This is consistent with the expectation that ionized impurity scattering is higher in the more highly doped samples.

However, as shown in Fig. 1(b), when μ_{sum} is plotted as a function of the sum of excess carrier density and the ionized dopant concentration, the curves for the highly doped samples are shifted to the right and align themselves with the lowly doped samples similarly to our previous paper. This indicates that dopants and excess carriers have a similar impact on the mobility. The p-type data also shift to the right and align with the n-type data from the previous study and form a continuous curve, within the measurement uncertainties.

The measurement results for other temperatures, ranging from -120 °C to 180 °C, are shown in Fig. 2. As above, the mobility sum forms a continuous curve when plotted against the sum of excess carrier density and the ionized dopant concentration. Fig.2 also shows that increased phonon (lattice) scattering produces a reduction of mobility as the temperature increases. This causes the mobility sum to become less dependent on carrier injection and doping. At room temperature, the p-type data align themselves with the n-type data from the previous study for all temperatures shown in Fig. 2.

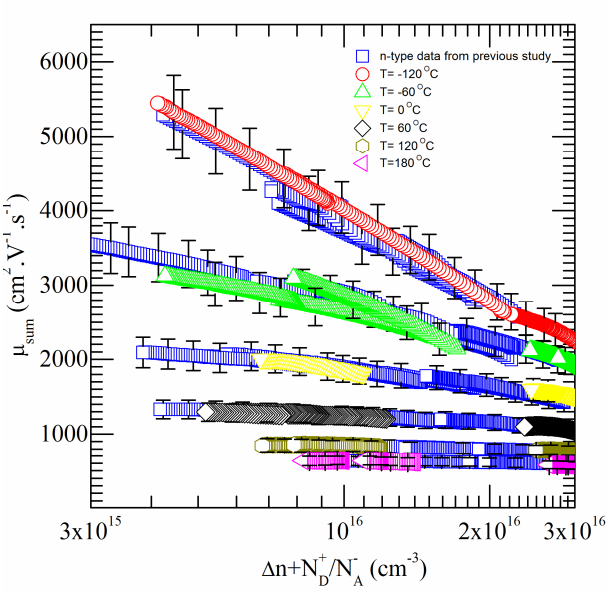

Fig. 2. Measured mobility sum as a function of the sum of excess carrier density and the ionized doping density at -120°C, -60°C, 0°C, 60°C, 120°C and 180°C.

IV. Empirical Model for the Mobility Sum

From the previous study, we have derived an empirical mobility sum model as a function of temperature, ionized dopant density, and carrier injection level by adopting the parameterization of μ_{sum} in the WCT-100 software used in the analysis of QSSPC lifetime measurements [18, 19].

The empirical model is derived by fitting the linearized relationship between the mobility sum data and sum of ionized dopant concentration and excess carrier density, $N_A^-+N_D^++\Delta n$ for every temperature. The linearized relationship is shown in equation 1 below.

$$\log\left(\frac{\mu_{sum}-\mu_{\min}}{\mu_{\max}-\mu_{sum}}\right)=-\alpha\log\left(N_A^-+N_D^++\Delta n\right)+\alpha\log\left(N_{ref}\right)+\log\left(\frac{1}{\beta}\right) \quad (1)$$

Where N_A^- is the ionized acceptor concentration, N_D^+ is the ionized donor concentration, Δn is the excess carrier density, and μ_{max}, β, α and N_{ref} are the parameters to be determined.

Figure 3 shows the n-type data from the previous study, and the new p-type data. At every temperature, the p-type data is in agreement with the n-type data. Therefore, the empirical model derived based on n-type samples is also applicable to p-type samples as a function of injection level and temperature from 150K to 450K. The empirical model derived previously is shown in equation (2).

$$\mu_{sum}=\mu_{\max 300K}\left(\frac{T}{300}\right)^{\gamma}+\frac{\left(\mu_{\min 300K}-\mu_{\max 300K}\right)\left(\frac{T}{300}\right)^{\gamma}}{1+\left(\frac{1}{\beta}\right)\left(\frac{N_{ref\,300K}}{N_A^-+N_D^++\Delta n}\right)^{\alpha}\left(\frac{T}{300}\right)^{\theta}} \quad (2)$$

Where $\mu_{max300K}$ is the maximum mobility sum at 300K, and γ is the temperature dependence power factor for μ_{max}. $N_{ref300K}$ is the total reference carrier concentration at 300K that takes the dopant impurity and carrier-carrier scattering into consideration, and affects the mobility sum mainly in the range of $N_A^-+N_D^++\Delta n$ that is comparable to it. θ is the temperature dependence power factor for N_{ref} . All the fitting parameters derived are listed in Table I.

TABLE I
PARAMETERS FOR MOBILITY SUM MODEL

Parameters	
$\mu_{max300K}$	1800 $cm^2 \cdot V^{-1} \cdot s^{-1}$
$N_{ref300K}$	$4.65\times10^{17} cm^{-3}$
β	8.36
α	0.97
γ	-2.28
θ	3.09

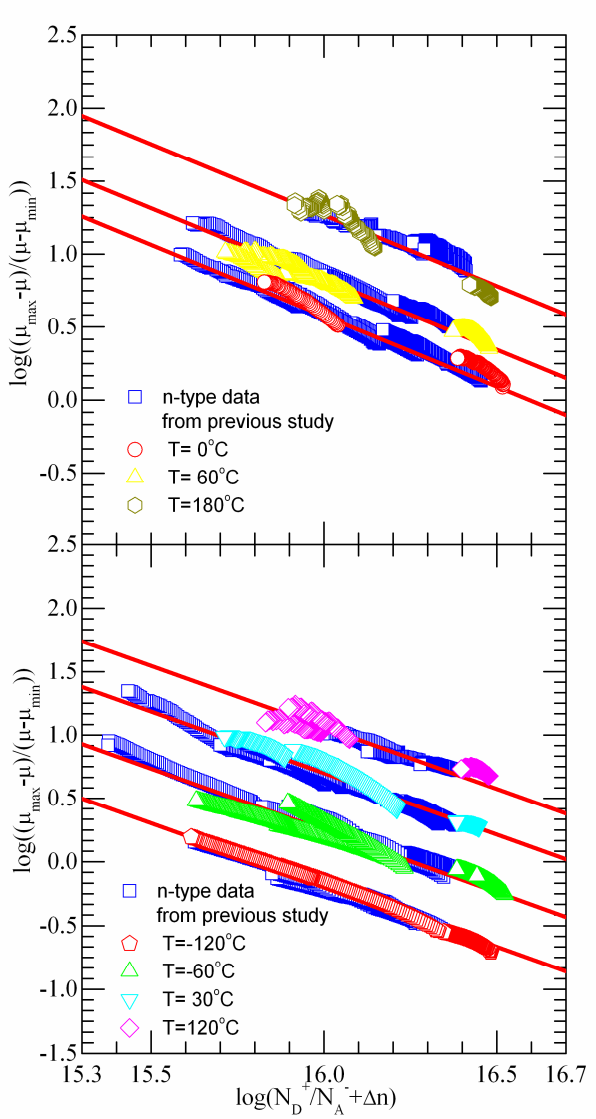

Fig. 3. Fitting of measured mobility sum using Equation (1) at -120°C, -60°C, 0°C, 30°C, 60°C, 120°C and 180°C. The symbols are calculated based on the left hand side of equation (1), the solid lines are the fitting using the right hand side of equation (1) by adjusting N_{ref} and α.

V. Comparison to Other Models

A. Applicability as a function of carrier injection

In this Section the empirical model is compared to other mobility models in order to assess its validity. Firstly, a comparison is made as a function of carrier injection level. Fig. 4 shows the resulting mobility sum from this study and the mobility models from WCT-100 parameterization, Klaassen [20-22], and Dorkel-Leturcq [23] with a doping density of $1\times10^{15} cm^{-3}$ (10Ω.cm *p*-type sample) at 300K in the $1\times10^{14} cm^{-3}$ to $3\times10^{16} cm^{-3}$ carrier injection range. The empirical model derived here from the photoconductance measurements is in good agreement with the existing injection dependence mobility models, especially in the range of injection levels relevant for the characterization of silicon wafers by photoconductance

measurements, that is, from approximately 1×10^{15}cm^{-3} to 3×10^{16}cm^{-3}. In this range, Eq. (2) gives intermediate values to the other models. Eq. (2) predicts a lower mobility sum than Klaassen's and WCT-100 parameterization, but it is close to the model of Dorkel-Leturcq beyond an injection level of 1×10^{16}cm^{-3}.

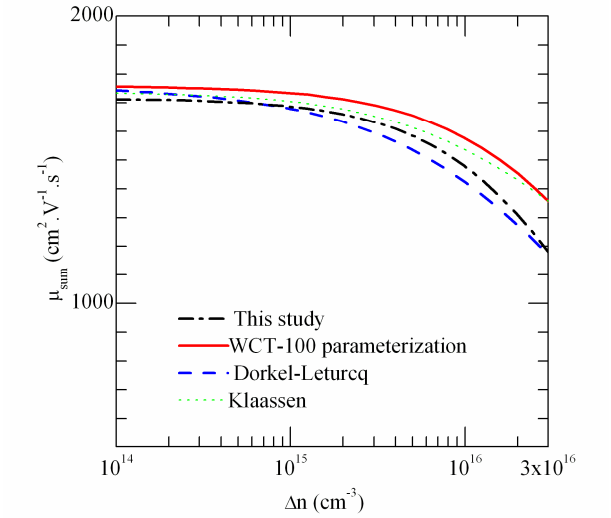

Fig. 4. Comparison of the empirical mobility sum from this study with the existing mobility models from WCT-100 parameterization, Klaassen and Dorkel-Leturcq as a function of injection at 300K for *p*-type silicon at doping density of 1×10^{15}cm^{-3}.

B. Modeling the Influence of Dopant Density

Fig. 5 shows the doping dependence of the mobility sum computed at 300K and at an injection level of 1×10^{16}cm^{-3}. The

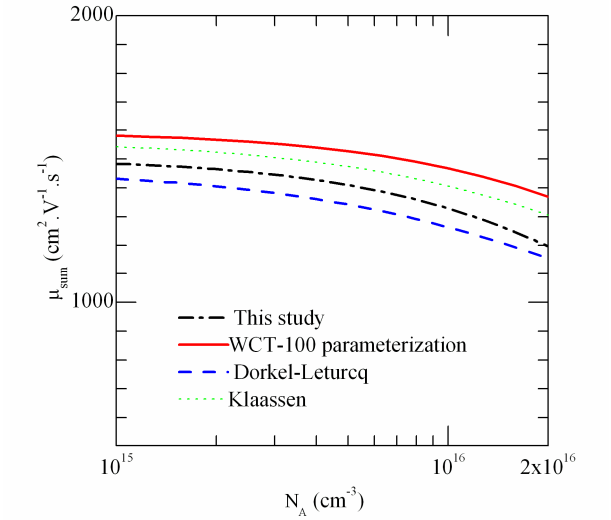

Fig. 5. Comparison of the empirical mobility sum from this study with the existing mobility models from WCT-100 parameterization, Klaassen and Dorkel-Leturcq as a function of doping density at 300K and injection level of 1×10^{16}cm^{-3} for *p*-type silicon.

mobility models from Klaassen, Dorkel-Leturcq and WCT-100 parameterization are included for comparison. The mobility predicted from our empirical model lies within the mobilities from other models and is in reasonable agreement with them, even if it is slightly lower at high dopant concentrations. The most heavily doped sample used in this experiment is $N_A=2\times10^{16}$cm^{-3}. Therefore the empirical model of Eq. (2) may not be valid for samples doped more than 2×10^{16}cm^{-3}.

C. Modeling the Influence of Temperature

Fig. 6 shows the modeled temperature dependence of the mobility sum from the empirical model together with the mobility models from Klaassen and Dorkel-Leturcq. WCT-100

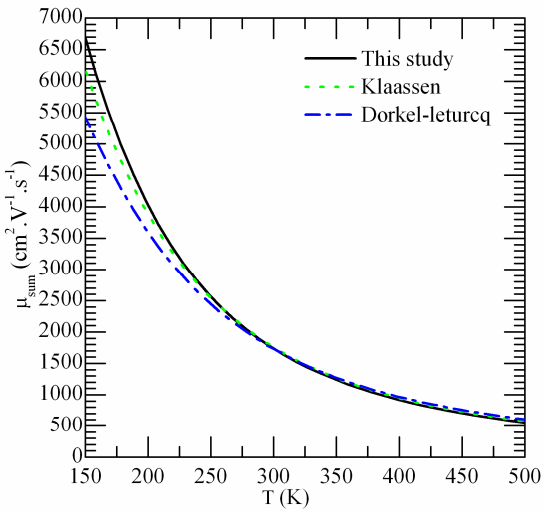

Fig. 6. Comparison of the empirical mobility sum from this study with the existing mobility models from Klaassen and Dorkel-Leturcq as a function of temperature at doping density of 1×10^{16}cm^{-3} and injection level of 1×10^{16}cm^{-3} for *p*-type silicon.

parameterization is not included as it does not include temperature dependence. The mobility sum is computed at a doping density of 1×10^{15}cm^{-3} and an injection level of 1×10^{15}cm^{-3}. The empirical model is in good agreement with both Klaassen's and Dorkel-Leturcq's models especially at high temperatures. The empirical model may not be valid at temperatures below 150K.

VI. Conclusion

In this paper, we validate the use of the recently derived empirical model based on n-type silicon data for p-type silicon of doping density from 1.3×10^{15} cm^{-3}(0.75Ω.cm) to 2×10^{16} cm^{-3} (10Ω.cm) as a function of injection level from 3×10^{15} cm^{-3} to 3×10^{16} cm^{-3} and temperature from 150K to 450K. The empirical model predicts stronger injection dependence at high injection level, and stronger doping dependence at high dopant

concentration than Klaassen's, Dorkel-Leturcq's and the WCT-100 parameterization. For *p*-type boron doped silicon, the empirical model is most accurate within a carrier injection range of 3×10^{15}cm^{-3} to 3×10^{16}cm^{-3}, doping density from 1.3×10^{15}cm^{-3} (10Ω.cm) to 2×10^{16}cm^{-3} (0.75Ω.cm) and temperature from 150K to 450K. The model may not be as accurate outside these ranges. We have verified that the model is also valid for p-type silicon at 300K. The model can be used for temperature and injection dependent lifetime measurements and to predict the conductance of the moderately injected bulk of high efficiency silicon solar cells. [24].

ACKNOWLEDGMENTS

This work has been supported by the Australian Research Council (ARC) and the Australian Renewable Energy Agency (ARENA) fellowships program.

REFERENCES

[1] S. Rein, T. Rehrl, W. Warta, and S. W. Glunz, "Lifetime spectroscopy for defect characterization: Systematic analysis of the possibilities and restrictions," *Journal of Applied Physics,* vol. 91, pp. 2059-2070, 2002.

[2] B. B. Paudyal, K. R. McIntosh, D. H. Macdonald, B. S. Richards, and R. A. Sinton, "The implementation of temperature control to an inductive-coil photoconductance instrument for the range of 0–230°C," *Progress in Photovoltaics: Research and Applications,* vol. 16, pp. 609-613, 2008.

[3] Irvin and J. C, "Resistivity of Bulk Silicon and of Diffused Layers in Silicon," *The Bell System Technical Journal* vol. 41, pp. 387-410, 1962.

[4] P. W. Chapman, O. N. Tufte, J. D. Zook, and D. Long, "Electrical Properties of Heavily Doped Silicon," *Journal of Applied Physics,* vol. 34, pp. 3291-3295, 1963.

[5] M. Finetti and A. M. Mazzone, "Impurity effects on conduction in heavily doped n-type silicon," *Journal of Applied Physics,* vol. 48, pp. 4597-4600, 1977.

[6] W. R. Thurber, R. L. Mattis, Y. M. Liu, and J. J. Filliben, "The Relationship between resistivity and dopant density for phosphorus- and boron-doped silicon " *National Bureau of Standards Special Publication 400-64,* 1981.

[7] E. Fourmond, M. Forster, R. Einhaus, H. Lauvray, J. Kraiem, and M. Lemiti, "Electrical properties of boron, phosphorus and gallium co-doped silicon," *Energy Procedia,* vol. 8, pp. 349-354, 2011.

[8] F. Schindler, M. C. Schubert, A. Kimmerle, J. Broisch, S. Rein, W. Kwapil, and W. Warta, "Modeling majority carrier mobility in compensated crystalline silicon for solar cells," *Solar Energy Materials and Solar Cells,* vol. 106, pp. 31-36, 2012.

[9] F. Dannhäuser, "Die abhängigkeit der trägerbeweglichkeit in silizium von der konzentration der freien ladungsträger—I," *Solid-State Electronics,* vol. 15, pp. 1371-1375, 1972.

[10] J. Krausse, "Die abhängigkeit der trägerbeweglichkeit in silizium von der konzentration der freien ladungsträger—II," *Solid-State Electronics,* vol. 15, pp. 1377-1381, 1972.

[11] D. H. Neuhaus, P. P. Altermatt, R. A. B. Sproul, A. Sinton, A. Schenk, A. Wang, and A. G. Aberle, "Method for measuring majority and minority carrier mobility in solar cells," in *Proceedings of the 17th European Photovoltaic Solar Energy Conference*, 2001, pp. 242-245.

[12] Z. Hameiri, T. Trupke, and R. Sinton, "Determination of Carrier Mobility Sum in Silicon Wafers by Combined Photoluminescence and Photoconductance Measurements," in *27th European Photovoltaic Solar Energy Conference and Exhibition*, 2012, pp. 1477 - 1481.

[13] P. Zheng, F. E. Rougieux, D. Macdonald, and A. Cuevas, "Measurement and Parameterization of Carrier Mobility Sum in Silicon as a Function of Doping, Temperature and Injection Level," *Photovoltaics, IEEE Journal of,* vol. 4, pp. 560-565, 2014.

[14] F. E. Rougieux, Z. Peiting, M. Thiboust, J. Tan, N. E. Grant, D. H. Macdonald, and A. Cuevas, "A Contactless Method for Determining the Carrier Mobility Sum in Silicon Wafers," *Photovoltaics, IEEE Journal of,* vol. 2, pp. 41-46, 2012.

[15] A. Richter, S. W. Glunz, F. Werner, J. Schmidt, and A. Cuevas, "Improved quantitative description of Auger recombination in crystalline silicon," *Physical Review B,* vol. 86, p. 165202, 2012.

[16] A. Cuevas, "Modelling silicon characterisation," *Energy Procedia,* vol. 8, pp. 94-99, 2011.

[17] J. Tan, D. Macdonald, F. Rougieux, and A. Cuevas, "Accurate measurement of the formation rate of iron–boron pairs in silicon," *Semiconductor Science and Technology,* vol. 26, p. 055019, 2011.

[18] P.P.Altermatt, J.Schmidt, M.Kerr, G.Heiser, and A.G.Aberle, "Exciton-enhanced auger recombination in crystalline silicon under intermediate and high injection conditions," in *16th European photovoltaics solar energy conference*, 2000, pp. 243-246.

[19] K. R. McIntosh and R. A. Sinton, "Uncertainty in photoconductance lifetime measurements that use an inductive-coil detector," in *23rd European Photovoltaic Solar Energy Conference*, Valencia, Spain, 2008, pp. 77-82.

[20] D. B. M. Klaassen, "A unified mobility model for device simulation," in *Electron Devices Meeting, 1990. IEDM '90. Technical Digest., International*, 1990, pp. 357-360.

[21] D. B. M. Klaassen, "A unified mobility model for device simulation—I. Model equations and concentration dependence," *Solid-State Electronics,* vol. 35, pp. 953-959, 1992.

[22] D. B. M. Klaassen, "A unified mobility model for device simulation—II. Temperature dependence of carrier mobility and lifetime," *Solid-State Electronics,* vol. 35, pp. 961-967, 1992.

[23] J. M. Dorkel and P. Leturcq, "Carrier mobilities in silicon semi-empirically related to temperature, doping and

injection level," *Solid-State Electronics,* vol. 24, pp. 821-825, 1981.
[24] P. J. Cousins, D. D. Smith, L. Hsin-Chiao, J. Manning, T. D. Dennis, A. Waldhauer, K. E. Wilson, G. Harley, and W. P. Mulligan, "Generation 3: Improved performance at lower cost," in *Photovoltaic Specialists Conference (PVSC), 2010 35th IEEE*, 2010, pp. 000275-000278.